Vehicle to grid from the Electric Vehicle point-of-view to reduce peak demand and system cost

Menendez Agudin, A.; Chandra Mouli, G.R.; Bauer, P.

DOI
10.1109/ESARS-ITEC60450.2024.10819878

Publication date
2025

Document Version
Final published version

Published in
2024 IEEE International Conference on Electrical Systems for Aircraft, Railway, Ship Propulsion and Road Vehicles and International Transportation Electrification Conference, ESARS-ITEC 2024

2024 IEEE International Conference on Electrical Systems for Aircraft, Railway, Ship Propulsion and Road Vehicles & International Transportation Electrification Conference (ESARS-ITEC) | 979-8-3503-7390-5/24/$31.00 ©2024 IEEE | DOI: 10.1109/ESARS-ITEC60450.2024.10819878

Vehicle to grid from the Electric Vehicle point-of-view to reduce peak demand and system cost

Alvaro Menendez-Agudin
Delft University of Technology
Delft, The Netherlands
A.M.A.MenendezAgudin@tudelft.nl

Gautham Ram Chandra Mouli
Delft University of Technology
Delft, The Netherlands
G.R.ChandraMouli@tudelft.nl

Pavol Bauer
Delft University of Technology
Delft, The Netherlands
P.Bauer@tudelft.nl

***Abstract*—The study presents Electric Vehicle (EV) Point-of-View (POV) Vehicle to Grid (V2G) optimisation, where the system knows the trips and energy demand of the EV. This allows it to be less conservative in the departure State of Charge (SoC) of the EV battery. The peak and cost reduction of Vehicle POV optimisation are compared with state-of-the-art Location Point-of-View optimisation, this is, the car can do V2G but it has to depart each location with at least 80% SoC as the next trip energy demand is unknown. A Mix Integer Linear Programming (MILP) V2G optimisation approach is presented to reduce peak demand and total system cost of a fleet of EVs travelling between several residential locations and one common workplace.**

Simulations were conducted with 26 EVs unevenly distributed between five residential locations and commuters to a common workplace. The results indicate little differences in the reduction of peak demand between both POVs of V2G optimisation. However, the system cost can be further reduced with Vehicle Point-of-View optimization, saving an additional 200 euros annually per household by transporting cheaper energy from workplaces to residential locations.

***Index Terms*—Electric Vehicle, Vehicle to Grid, Peak Reduction**

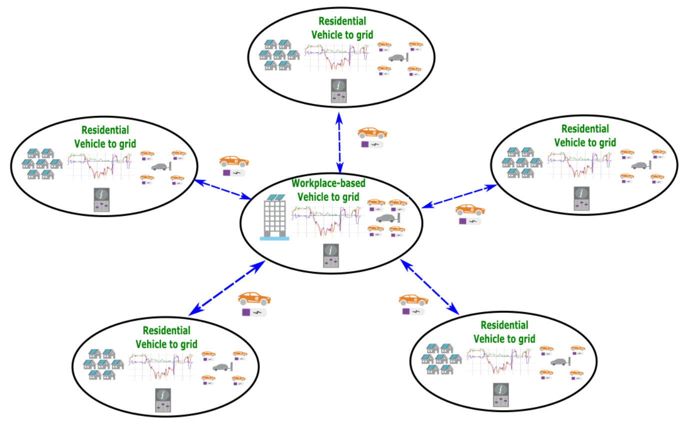

Fig. 1: Diagram of the system

I. Introduction

Electrification of mobility to reduce GHG emissions is a growing trend, and a large increase in EV uptake is expected in the coming years, [1]. Although this electrification is needed, uncoordinated charging of EVs in a distribution grid can lead to local grid problems [2]. Transportation is not the only sector electrified, as the installation of heat pumps to electrify the heating and the installation of photovoltaic generation also have an impact on the grid [3]. However, the electric vehicle acts as a different electric load, one that serves as a mobile storage unit capable of contributing to load management within the power grid through Smart Charging to reduce grid congestion, [4], or even bidirectional Vehicle-to-Grid (V2G), [5]. On the other hand, if EV charging is left uncontrolled, increased demand can negatively impact the power grid, [6].

V2G can be used to provide services to the grid such as frequency regulation, [7], decrease voltage deviations and power loss, [8], reduce grid congestion, [9], and overall increase grid safety and reliability, [10]. When optimising the (dis)charging patterns of EVs in a V2G scenario, EV availability is a key factor, as storing energy in the EV battery or discharging via V2G can only be done when the EV is connected. Some studies consider this issue and make a forecast of the expected availability of EVs, [11], or study the effect of EV availability in a charging pool on the V2G services, [12]. A similar study of the impact of the availability of shared EVs to provide peak reduction to a commercial building is studied in [13]. These studies focus on optimising the location power demand, considering the EV as another asset that can or cannot be connected. The lack of information about the electric vehicle's next trip makes the charging optimization algorithms conservative so the EV does not run out of battery, [14]. Similar studies such as [15] and [16] use EV users' input of expected departure time and desired departure SoC. In the latter, they compared how different departure SoC and charging rates influence the daily payments in the real-time pricing charging optimisation.

Vehicle to Grid studies often focus on Location POV V2G, this is, the car can do V2G with the added constraint that it has to depart each location with at least 80% SoC. This simulates the most common scenario in the literature, where the system only has knowledge about the EV when it is connected to the Charging Station. After that the system does not know what the car is going to do, so it charges almost all the battery in case it is needed. Location POV V2G is compared with the Vehicle POV V2G presented in this paper, where the Point of View is changed to the EV. This change allows the EV to plan according to the energy prices, charger availability at each location, and energy used for driving during the week. By doing this, the EV can charge the battery to low SoC if the destination has better prices or excess PV generation that can be used to charge the EV at lower prices.

II. MILP Formulation

The following section describes the formulation used to solve the problem. A Mix Integer Linear Programming (MILP) optimisation has been used to reduce the peak demand of all residential locations and workplace and to reduce the overall system cost.

A total of seven decision variables have been used, $P_{ch_{kt}}$ and $P_{V2G_{kt}}$ that set the charging and discharging power of each EV k over time t respectively. P_{r}^{Max} and P_{w}^{Max} set the contracted power, this is the peak demand in each residential location and work, respectively. Three binary variables were used to limit the possibility of charging and discharging the car at the same time, $Bi_{ch_{kt}}$, or to limit that power cannot be fed and drawn from the grid at the same time in residential, $Bi_{G_{rt}}$, and workplace, $Bi_{G_{wt}}$, locations. All of the variables used in the problem are positive.

A. Objective functions

The MILP formulation used in this study aims to reduce the peak demand at home and work while reducing system costs for all users. All locations have different load and photovoltaic generation profiles but all of them have the same energy prices, except in the high prices scenarios. Two different objective functions of the MILP formulation are formulated. The first, shown in Equation (1), applies a weight factor N to P_{r}^{Max} and P_{w}^{Max} to make the objective binding and reduce the peak demand as the main objective. The second, shown in Equation (2), implements a linearised cost of grid capacity in the function obtained from [17]. In this case, it may be more profitable to invest extra in higher grid capacity if the profits from buying and selling energy can overcome this initial investment. The parameters R_{r} and R_{w} are the revenue obtained by selling energy in residential locations, Equation (3), and on the workplace, Equation (4), respectively. This formulation was used to keep the problem linear and avoid using a multiobjective formulation.

$$\max \quad R_{\mathrm{r}} + R_{\mathrm{w}} - (P_{\mathrm{r}}^{\mathrm{Max}} + P_{\mathrm{w}}^{\mathrm{Max}})N \tag{1}$$

$$\max \quad R_{\mathrm{r}} + R_{\mathrm{w}} - (\lambda(P_{\mathrm{r}}^{\mathrm{Max}} + P_{\mathrm{w}}^{\mathrm{Max}}) - \gamma) \tag{2}$$

$$R_{\mathrm{r}} = \sum_{r=1}^{R}\sum_{t=1}^{T} P_{\mathrm{feed}_{rt}}\Delta t C_{rt} S_c - P_{\mathrm{drawn}_{rt}}\Delta t C_{rt} \tag{3}$$

$$R_{\mathrm{w}} = \sum_{t=1}^{T} P_{\mathrm{feed}_{wt}}\Delta t C_{wt} S_c - P_{\mathrm{drawn}_{wt}}\Delta t C_{wt} \tag{4}$$

$P_{\mathrm{feed}_{rt}}$ and $P_{\mathrm{drawn}_{rt}}$ are the power supplied and drawn to/from the grid, respectively, at each residential location, r, and timestep, t. The same formulation is used for work, with the difference that all electric vehicles are connected to the same workplace, while connected to R different residential neighbourhoods, as shown in Figure 1. The timestep duration, Δt, is 15 minutes. The electricity cost is represented by C_{rt}, and a selling factor is applied to indicate that the selling cost is lower than the buying one, S_c.

B. Electric Vehicle Constraints

The state function of the EV state of charge and its constraints are defined as:

$$\mathrm{SoC}_{kt+1} = \mathrm{SoC}_{kt} + \frac{P_{\mathrm{ch}_{kt}}\Delta t}{Q_{\mathrm{k}}}\eta_{\mathrm{ch}} - \frac{P_{\mathrm{V2G}_{kt}}\Delta t}{Q_{\mathrm{k}}\eta_{\mathrm{V2G}}} - \frac{P_{\mathrm{D}_{kt}}\Delta t}{Q_{\mathrm{k}}} \tag{5}$$

$$Av_{rkt} = \begin{cases} 1 & rkt \in [rkt_{arr};\ rkt_{dep}] \\ 0 & \text{otherwise} \end{cases} \tag{6}$$

$$0.1 \leq \mathrm{SoC_{kt}} \leq 0.9 \tag{7}$$

$$\mathrm{S}oC_{kt_{dep}} \geq 0.8 \tag{8}$$

$$P_{\mathrm{ch}_{kt}} \leq P_{\mathrm{ch_{kt}}}^{\max} Av_{rkt}(1 - Bi_{ch_{kt}}) \tag{9}$$

$$P_{\mathrm{V2G}_{kt}} \leq P_{\mathrm{V2G_{kt}}}^{\max} Av_{rkt} Bi_{ch_{kt}} \tag{10}$$

Where SoC_{kt} is the state of charge of the Electric Vehicle k at timestep t; Q_k the battery energy capacity of the EV and η_{ch} and η_{V2G} the charging and discharging efficiencies, respectively. The energy used by the car for driving is represented by $P_{\mathrm{D}_{kt}}\Delta t$, where a constant average demand power has been considered for each trip timestep. Trip times and energy are not decision variables, but inputs for the problem.

Equation (6) sets the availability of a car connected to the charging station at each location, having the ability to provide V2G services. Equation (8) is only included in the Location POV problem. In the Electric Vehicle POV V2G formulation, this constraint is removed so the EV can depart with a lower SoC from a location to charge cheaper energy at the next. This small change gives the optimisation more freedom to choose not only the better time but also the better place to (dis)charge the EV to reduce costs.

Equations (9) and (10) specify that the vehicle can only charge or discharge if the EV k is connected at time t at the location r, if $Av_{rkt} = 1$. It also limits the maximum charging and discharging power, $P_{\mathrm{ch}_{kt}}^{\max}$ and $P_{\mathrm{V2G}_{kt}}^{\max}$ and cannot charge and discharge at the same time, using the binary variable $Bi_{ch_{kt}}$.

C. Grid Constraints

The grid constraints needed for the problem were formulated as follows:

$$P_{L_{rt}} - P_{PV_{rt}} + P_{ch_{kt}} - P_{V2G_{kt}} = P_{draw_{rt}} - P_{feed_{rt}} \quad (11)$$

$$P_{L_{wt}} - P_{PV_{wt}} + P_{ch_{kt}} - P_{V2G_{kt}} = P_{draw_{wt}} - P_{feed_{wt}} \quad (12)$$

Equations (11) and (12) are the equations of power balance for residential locations and workplace, respectively. The load demand at each location and at the workplace is represented by $P_{L_{rt}}$ and $P_{L_{wt}}$, respectively, while the generated photovoltaic energy is represented by $P_{PV_{rt}}$ and $P_{PV_{wt}}$, respectively. As all the variables are positive, it is important to set the signs correctly in the balance equation. In this case, all power flowing into the building, $P_{PV_{rt}}$, $P_{V2G_{kt}}$ and $P_{feed_{rt}}$ have a negative sign, while the power flowing from the building to the loads or the grid, $P_{L_{rt}}$, $P_{ch_{kt}}$ and $P_{draw_{rt}}$ have a positive sign, as can be seen in Figure 2.

$$P_{\mathrm{draw}_{rt}} \leq P_{\mathrm{r}}^{\mathrm{Max}} \quad (13)$$

$$P_{\mathrm{r}}^{\mathrm{Max}} \leq P_{\mathrm{grid}}^{\max}(1 - Bi_{G_{rt}}) \quad (14)$$

$$P_{\mathrm{feed}_{rt}} \leq P_{\mathrm{grid}}^{\max} Bi_{G_{rt}} \quad (15)$$

$$P_{\mathrm{draw}_{wt}} \leq P_{\mathrm{w}}^{\mathrm{Max}} \quad (16)$$

$$P_{\mathrm{w}}^{\mathrm{Max}} \leq P_{\mathrm{grid}}^{\max}(1 - Bi_{G_{wt}}) \quad (17)$$

$$P_{\mathrm{feed}_{wt}} \leq P_{\mathrm{grid}}^{\max} Bi_{G_{wt}} \quad (18)$$

Equations (14) and (15) used the binary variable $Bi_{G_{rt}}$ to constrain that power cannot be fed and drawn from the grid at the same time and that power must be lower than the grid capacity, $P_{\mathrm{grid}}^{\max}$. The peak demand, P_{r}^{Max} and P_{w}^{Max} must be lower than the installed grid capacity, as explained in Equations (14), (15), (17) and (18). The same approach is used for the workplace constraints. The binary variables are used so that the problem can be linear, and a MILP optimisation can be used, thus reducing computational cost.

III. Case Studies

The MILP formulation previously described was applied to three different scenarios. High work PV, where the workplace has excess PV generation that the EVs can use to charge the battery. High home and work prices, where home and work prices are twice the original wholesale market price, respectively. Energy prices have been taken from the Netherlands wholesale energy market in 2023.

All scenarios have been calculated with both objective functions. First, the simulations are run with the weight factor being a high enough number to make peak reduction the main objective Equation (1). Secondly, the weight factor has been changed to represent the linear cost of installed capacity, Equation (2), where λ equals 81.6 and γ equals 471.8. The first case will focus on supporting the grid with peak reduction, while the second one will focus on minimising system costs exclusively.

Simulations were carried out with 26 EVs commuting between a common workplace and their homes. For simplification, the workplace and five different residential locations were considered separate nodes. The study focuses on people who work in the same location but live in different places. It has been considered that all 26 EVs commute and are then parked at work, but only 10, 7, 5, 3 and 1 cars are available at each of the residential locations, respectively. All EVs have a charger available at home and work, but only 50% of them are bidirectional at work and 75% at home, being able to discharge energy when needed.

All simulations are conducted using a base case scenario of Location POV V2G, where the car can perform V2G but must leave each location with at least 80% SoC. This simulates the common scenario in the literature, where the system only has information about the EV when it is connected to the charging station. Beyond that, the system cannot predict the car's behaviour, so it ensures the battery is charged to at least 80% SoC in case it is needed. Location POV V2G is compared to the Vehicle POV V2G approach presented in this paper, which shifts the perspective to the EV itself. This shift allows the EV to plan based on energy prices, charger availability, and energy usage for driving throughout the week. If the vehicle anticipates having access to a charger at work with lower energy prices, it can depart home with a low SoC, taking advantage of cheaper charging.

The Simulations were conducted using real data from anonymous household consumption and generation in summer and scaled up so each residential location is composed of 100 houses with 20% of them having PV generation. The work profile used is a normalized standard profile with the yearly demand of the Applied Sciences building at TU Delft University. The closest parking has 300 parking spots, so 26 charging points is a reasonable 10% EV penetration.

IV. Results

All scenarios have been simulated for three days using the Pyomo package in Python and the linear solver GLPK. Results for peak demand and total cost have been obtained for each scenario, objective function, and V2G mode.

A two-day example of the power curves from residential location 1, the one with 10 EVs, can be seen in Figure 2 for both V2G modes. Charging P_{ch_t} and discharging P_{V2G_t} powers shown in the plot are the summation of the charging and discharging powers of the 10 EVs. The energy change with the grid, represented as P_{grid_t} is equal to P_{draw_t} minus P_{feed_t} as shown in the power flows Equation (11). The plot shows the high home price scenario with the cost objective function, (2).

It shows the EV fleet (dis)charging power adapting to the Load Demand and PV generation. The grey areas show the working hours, where cars are not connected at home and cannot provide V2G services. The (dis)charging curves in the grey areas of Figure 2 are due to different departure and arrival times of each EV. The yellow areas show when the EVs are connected at home, thus providing V2G services. In both V2G modes the (dis)charging patterns are very similar in the evening hours, as the cars come from the workplace with energy in the battery and discharge it to reduce the demand in the evening hours when the price is higher.

The arrival times of the EVs are not the same, so even if some of them may arrive early in the afternoon, others arrive later in the evening. This is reflected in the plot as the discharging power ramps up slowly at first, from 18 to 20 hours, until all EVs are connected when it has a peak in discharging power, between 20 to 22 hours, to sell energy at high evening prices.

The main difference between Figure 2a and 2b can be seen in the last hours of the home connection period, before departing to work. In the Location POV V2G, the cars are forced to depart with at least 80% SoC, as explained in Equation (8), which forces the car to charge when the price is lower, in the last hours, to obey this constraint. In the Vehicle POV V2G this constraint is removed, so the cars can depart from home with lower SoC to charge at cheaper prices at work. This reduces the charging needs of the EVs at home, reducing the demand at home and the overall cost of the system.

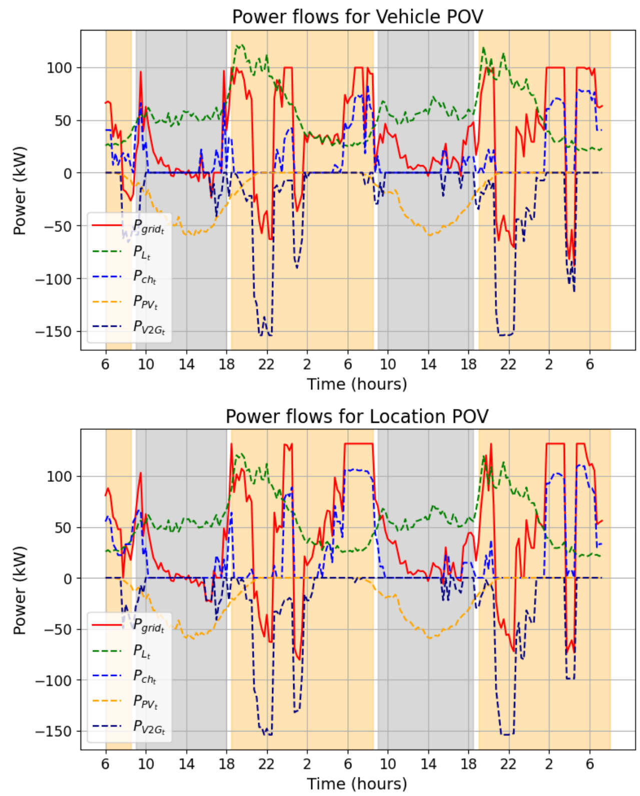

Fig. 2: Residential Location 1 Power curves for different POV

This distinction can be better seen in Figure 3, where the (dis)charging patterns and the SoC of a vehicle are plotted for both V2G modes in the high home prices scenario. As can be seen in the Vehicle POV V2G Figure 3 a, the electric vehicle does most of the charging at work, where the price is lower, and most of the discharging at home, where the price is higher. Not only that, the car leaves with low SoC levels from home, so it can charge the battery as much as possible with cheaper energy at work. It departs work with 90% SoC all three days while it departs home with close to 10% SoC, the higher and lower limits, respectively. This occurs because the system has perfect knowledge of the trip energy consumption so it can depart with just enough energy to arrive at work with 10% SoC.

On the other hand, Location POV V2G is forced to leave each location with 80% SoC, so it charges the EV during the night when prices are the lowest during the home period, although still higher than the work prices. It is important to remember that not all cars have a bidirectional charger available, so not all cars can charge all days at work and discharge all days at home. Although this study does not consider battery degradation caused by extra battery cycling while providing V2G services, it is something that should be considered. The ageing of the battery as an additional cost implemented in the optimisation itself is studied in [18]. Frequent high Depth of Discharge charging and discharging of the EV battery as can be seen in 3 can be very detrimental to the battery, greatly increasing its ageing, [19].

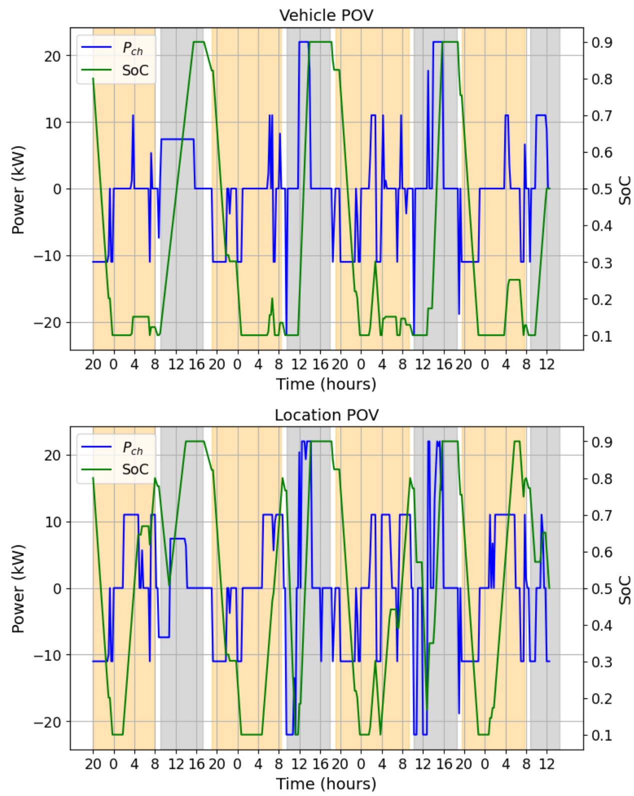

Fig. 3: Charging patterns of one EV in different V2G modes.

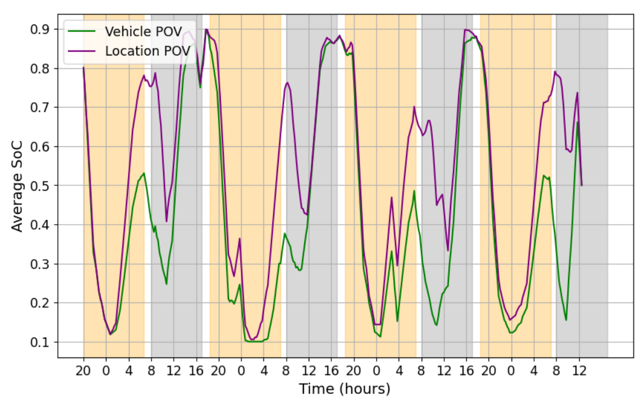

Fig. 4: Average SoC of the fleet in different V2G modes.

Figure 4 shows the average SoC of the 10 EVs in residential location 1. As explained before, it can be seen how cars charge as much as possible at work, where the energy is cheaper, and then discharge it once they arrive home, at the peak price of the evening hours. This (dis)charging pattern means that the fleet of EVs is effectively using their batteries to transport cheap energy from work back into residential locations where the prices are higher. It is after this discharge has occurred that the differences can be spotted, as in the Location POV V2G the cars are forced to charge to higher SoC, as can be seen in the figure.

Figure 5 shows the peak reduction for each scenario and target. The peak reduction is calculated following Equation (19). Where α_i represents the peak reduction in each scenario and P_{BaU} and P_{Opt} the peak demand in the business as usual scenario, without EVs, and the optimised scenario respectively. The figure shows box plots with the peak reduction of all residential locations and its average.

With the use of boxplots, the difference between the residential locations can be better seen, as the number of EVs in each location; 10, 7, 5, 3 and 1 respectively, greatly affects the peak reduction.

$$\alpha_i = \frac{P_{BaU} - P_{Opt}}{P_{BaU}} \times 100 \tag{19}$$

As can be seen in Figure 5, all scenarios with the peak reduction as the objective were able to reduce the average peak, blue line of each box, further with Vehicle POV V2G than with Location POV V2G. However, in all the scenarios the maximum and minimum peak reduction achieved is the same in both V2G modes, the upper and lower lines of each box. This corresponds to residential location 1, the one with 10 EVs, and residential location 5, the one with 1 EV, respectively. This shows that after a certain number of EVs the Location POV has the same peak reduction as the Vehicle POV. As explained in Figure 3, the EVs are arriving home with high SoC levels, so energy is available for discharge at the evening peak demand. EVs charging during the night to depart with 80% SoC have little or no effect on the reduction of peak demand, as at night the load is low enough.

When the objective was to reduce the total cost considering the contracted power, Equation (2), only the scenario of high home price shows a higher peak reduction in Vehicle POV V2G. With higher home prices the system tries to discharge at home as much as possible, reducing peak demand.

Cost reduction comparison is shown in Figure 6. The cost reduction is calculated following Equation (20). Where β_i represents the cost reduction difference between V2G modes, C_L is the Location POV V2G total system cost and C_V is the Vehicle POV V2G system price.

$$\beta_i = \frac{C_L - C_V}{C_L} \times 100 \tag{20}$$

Figure 6 shows how much the total cost in the system has been reduced with the EV point-of-view optimization related to the location point of view. It can be seen how Vehicle POV V2G can reduce the cost further than Location POV V2G in all scenarios and with both objective functions. Removing the departure SoC constraint, (8), the optimization can select not only the optimal time but also the optimal place to charge as cheaply as possible and reduce system costs.

The total demand of the five residential locations during the study period is 1.5 times the total demand at work; thus the biggest cost difference occurs in the high home prices scenario. As more EVs can be discharged at home due to the higher penetration of the bidirectional charger, more energy can be discharged at residential locations, reducing the overall cost of the system. The scenario with high PV at work presents the lowest difference as that scenario does not have the extreme prices used in the other two scenarios.

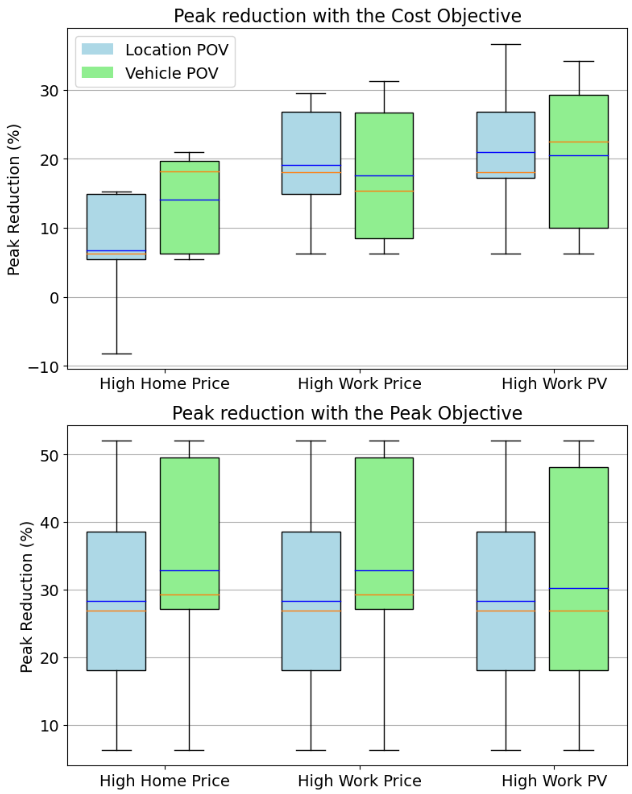

Fig. 5: Peak Reduction (%) by scenario and objective.

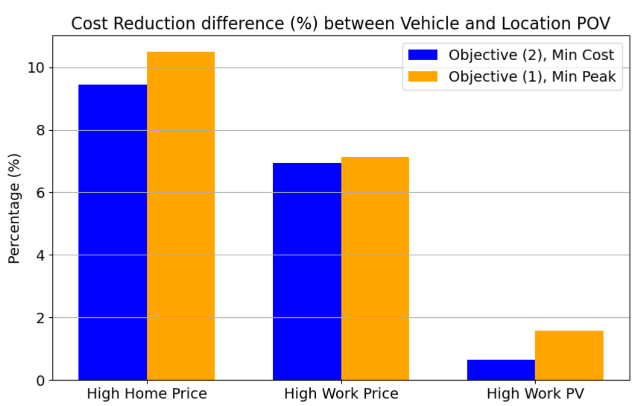

Fig. 6: Cost reduction comparison between V2G modes.

However, the high-photovoltaic scenario still saved 823 EUR in 3 days with only 26 EVs just by changing the optimisation POV to the vehicle instead of the location. If the savings are shared between the 500 homes in all residential locations, each home will have 200 euros extra at the end of the year.

V. Conclusions

The paper studies the benefits of changing the point of view from the Location, where the system only has knowledge about the EV when it is connected to the Charging Station, to the EV, where the EV can plan according to the energy prices, charger availability at each location and energy used for driving during the week. The information obtained with vehicle travel patterns and energy use can be used to further increase the benefits of V2G. Peak demand and system cost are minimised by implementing two different objective functions, one with cost reduction and one with peak reduction as the main objective, and results are compared with both points of view V2G optimisations.

Although electric vehicle charging patterns show that they take advantage of price differences between home and work charging, the achieved peak demand reduction is the same as 10% of households having an electric vehicle when peak demand reduction is set as the main objective. As EVs arrive home with high SoCs in both POVs optimization, peak demand does not present significant changes.

In scenarios with highly different prices between locations, the difference in total system cost was reduced between 7 and 10. 5% during the 3-day test period. However, these results were not achieved in the scenario with the same prices, where less than 1% difference was achieved. However, this small difference, obtained with only 26 EVs, accounts for 200 euros saved by each of the 500 households, 100 per residential location, a year.

VI. Acknowledgements

This research was funded by The Netherlands Organisation for Scientific Research (NWO) for the Flexible Energy Communities: Coupling e-mobility and Energy Communities (FlexECs) project.

References

[1] C. Tang, A. Tukker, B. Sprecher, and J. M. Mogollón, "Assessing the european electric-mobility transition: Emissions from electric vehicle manufacturing and use in relation to the eu greenhouse gas emission targets." *Environ Sci Technol*, vol. 57, no. 1, pp. 44–52, 2023.

[2] K. Clement-Nyns, E. Haesen, and J. Driesen, "The impact of vehicle-to-grid on the distribution grid," *Electric Power Systems Research*, vol. 81, no. 1, pp. 185–192, 2011. [Online]. Available: https://www.sciencedirect.com/science/article/pii/S0378779610002063

[3] N. Damianakis, G. R. C. Mouli, P. Bauer, and Y. Yu, "Assessing the grid impact of electric vehicles, heat pumps pv generation in dutch lv distribution grids," *Applied Energy*, vol. 352, p. 121878, 2023.

[4] M. Verhoog, N. Brinkel, and T. Alskaif, "Congestion management in lv grids using static and dynamic ev smart charging," in *2020 International Conference on Smart Energy Systems and Technologies (SEST)*, 2020, pp. 1–6.

[5] Y. Zhou and X. Li, "Vehicle to grid technology: A review," in *2015 34th Chinese Control Conference (CCC)*, 2015, pp. 9031–9036.

[6] E. Veldman and R. A. Verzijlbergh, "Distribution grid impacts of smart electric vehicle charging from different perspectives," *IEEE Transactions on Smart Grid*, vol. 6, no. 1, pp. 333–342, 2015.

[7] H. Liu, J. Qi, J. Wang, P. Li, C. Li, and H. Wei, "Ev dispatch control for supplementary frequency regulation considering the expectation of ev owners," *IEEE Transactions on Smart Grid*, vol. 9, no. 4, pp. 3763–3772, 2018.

[8] M. Singh, I. Kar, and P. Kumar, "Influence of ev on grid power quality and optimizing the charging schedule to mitigate voltage imbalance and reduce power loss," in *Proceedings of 14th International Power Electronics and Motion Control Conference EPE-PEMC 2010*, 2010, pp. T2–196–T2–203.

[9] M. A. López, S. Martín, J. A. Aguado, and S. De La Torre, "V2G strategies for congestion management in microgrids with high penetration of electric vehicles," *Electric Power Systems Research*, vol. 104, pp. 28–34, 2013.

[10] M. Yilmaz and P. T. Krein, "Review of the impact of vehicle-to-grid technologies on distribution systems and utility interfaces," *IEEE Transactions on Power Electronics*, vol. 28, no. 12, pp. 5673–5689, 2013.

[11] J. D. Fitzsimmons, S. J. Kritzer, V. A. Muthiah, J. J. Parmer, T. J. Rykal, M. T. Stone, M. C. Brannon, J. P. Wheeler, D. L. Slutzky, and J. H. Lambert, "Simulation of an electric vehicle fleet to forecast availability of grid balancing resources," in *2016 IEEE Systems and Information Engineering Design Symposium (SIEDS)*, 2016, pp. 205–210.

[12] E. Blasius, E. Federau, Z. Leonowicz, and P. Janik, "Assessment of e-vehicles availability in charging pool for support services in smart grids: Case study based on real data," in *17th IEEE International Conference on Environment and Electrical Engineering*. Institute of Electrical and Electronics Engineers Inc., 7 2017.

[13] A. M. Agudin, K. Jaikumar, G. R. C. Mouli, D. Slaifstein, J. Pool, and P. Bauer, "Impact of shared electric vehicles availability to provide peak reduction through vehicle-to-grid. a case study," in *IECON 2023- 49th Annual Conference of the IEEE Industrial Electronics Society*, 2023, pp. 1–6.

[14] K. N. Kumar, B. Sivaneasan, P. H. Cheah, P. L. So, and D. Z. W. Wang, "V2g capacity estimation using dynamic ev scheduling," *IEEE Transactions on Smart Grid*, vol. 5, no. 2, pp. 1051–1060, 2014.

[15] M. Honarmand, A. Zakariazadeh, and S. Jadid, "Optimal scheduling of electric vehicles in an intelligent parking lot considering vehicle-to-grid concept and battery condition," *Energy*, vol. 65, pp. 572–579, 2014.

[16] U. ur Rehman and M. Riaz, "Real time controlling algorithm for vehicle to grid system under price uncertainties," in *2018 1st International Conference on Power, Energy and Smart Grid (ICPESG)*, 2018, pp. 1–7.

[17] Stedin. (2024) Tarieven. Accessed on April 2024. [Online]. Available: https://www.stedin.net/tarieven/download-tarieven

[18] D. Slaifstein, J. Alpízar-Castillo, A. M. Agudin, L. Ramírez-Elizondo, G. R. C. Mouli, and P. Bauer, "Aging-aware battery operation for multicarrier energy systems," in *IECON 2023- 49th Annual Conference of the IEEE Industrial Electronics Society*, 2023, pp. 1–8.

[19] W. Vermeer, G. R. Chandra Mouli, and P. Bauer, "A comprehensive review on the characteristics and modeling of lithium-ion battery aging," *IEEE Transactions on Transportation Electrification*, vol. 8, no. 2, pp. 2205–2232, 2022.